New Soft-Switching Current Source Inverter for a Photovoltaic Power System

Byung-Moon Han*, Hee-Jung Kim* and Seung-Taek Baek*

Abstract - This paper proposes a soft-switching current source inverter for a photovoltaic power system. The proposed inverter has an H-type switched-capacitor module composed of two semiconductor switches, two diodes, and an LC resonant circuit. The operation of the proposed system was analyzed by a theoretical approach with equivalent circuits and was verified by computer simulations with SPICE and experimental implementation with a hardware prototype. The proposed system could be effectively applied for the power converter of photovoltaic power system interconnected with the AC power system.

Keywords: soft-switching CSI(current source inverter), photovoltaic system, PWM (pulse width modulation), IGBT (insulated-gate bipolar transistor), SPICE (simulation program with integrated circuit emphasis)

1. Introduction

The photovoltaic power system has been regarded the most promising of all future alternative energy sources. However, cost is still a key issue. One method to reduce the cost is to increase the efficiency of the power converter, because it is indispensable for interfacing the photovoltaic cells with the commercial power system and load.

Many studies have been conducted to develop a high-performance power converter for the photovoltaic power system[1]. Voltage source inverter has been normally used as a power converter for the photovoltaic power system, although the photovoltaic cell has characteristics of both the voltage source and current source[2]. Mainly because the voltage source inverter has higher efficiency than the current source inverter, due to the low dissipative losses in the DC link capacitor compared with the resistive and core losses in the DC link reactor. Lately, many researchers proposed have a soft-switching power converter to improve the efficiency of current source inverter[3,4].

In this paper, a new current source inverter with a soft-switching scheme is introduced for the photovoltaic power system. The basic idea is that the power converter using a soft-switching current source inverter could have a higher efficiency than the power converter using a hard-switching voltage source inverter[5]. The system is composed of a single-phase current source inverter with an H-type soft-switching module. The operation of the proposed system was analyzed in detail through theoretical approaches with equivalent circuit and computer simulations with SPICE. A scaled prototype was built and tested for verifying the feasibility of hardware implementation.

2. System concept

A current source inverter applied to the photovoltaic power system provides the following advantages:

• Utilization of the current limiting characteristic of the photovoltaic cell for safe operation, due to the low short circuit current of $1.1 \sim 1.3$ times the nominal current.

• No concern regarding the inrush current due to the short circuit of load and the short circuit of inverter due to the fault.

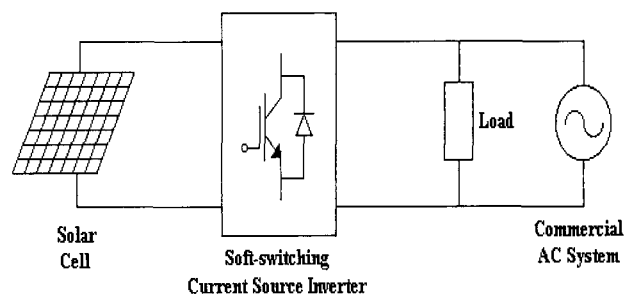• No requirement that the inverter output voltage higher than the power system voltage for interconnection.

Fig. 1 Concept for photovoltaic application

* The authors are with the Dept. of Electrical Engineering, Myongji University, Yongin 449-728, Korea(Dr. Han can be reached at erican@mju.ac.kr.)

The whole system concept for the proposed photovoltaic power system is shown in Fig. 1. The major component of the system is the soft-switching current source inverter, which interfaces the solar cell output with the commercial AC load and power system.

3. Current source inverter

The proposed soft-switching current source inverter has a single-phase current source inverter with a commutation circuit in the DC side as shown in Fig. 2.
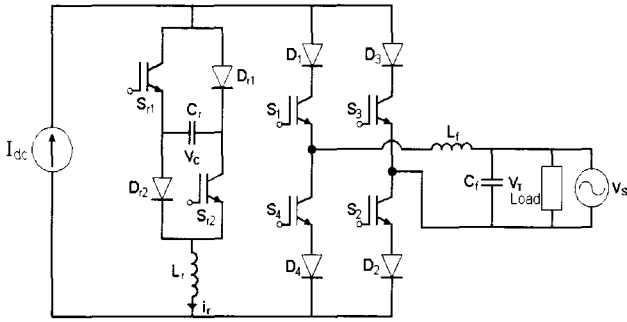

Fig. 2 Proposed current source inverter

The single-phase full bridge inverter consists of four IGBTs connected in series with four fast recovery diodes ($S_1/D_1 \sim S_4/D_4$). The soft-switching module consists of inductor L_r and capacitor C_r, IGBT S_{r1} and S_{r2}, and fast-recovery diode D_{r1} and D_{r2}. However, the power ratings of these IGBTs and diodes are much smaller than those in the full bridge.

The commutation process of the proposed system is divided into six operation modes. Fig. 3 shows waveforms of inductor current i_r, capacitor voltage v_C, voltage across main switches S_1 and S_3, and voltage across auxiliary switches S_{r1} and S_{r2} in the commutation circuit. Fig. 4 shows equivalent circuits for six operation modes. Each operation mode was explained in detail using a step by step approach.
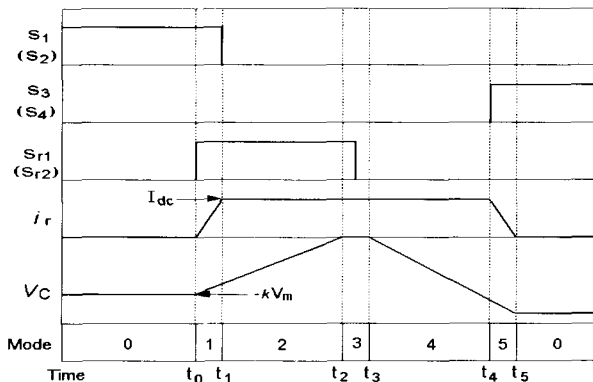

Fig. 3 Commutation operation diagram

Mode 0 – Initial state mode

The main current is assumed to be flowing through inverter switches S_1 and S_2 and the resonant current is zero. The capacitor C_r was already charged by $-kV_m$, where k is an initial charge factor equal to about 1.3 and V_m is the peak AC voltage.

Mode 1 – Current build-up mode

Commutation switches S_{r1} and S_{r2} turn on in a zero current state. The resonant current i_r starts to conduct and increases up to nominal reactor current I_{dc}. At the end of this mode, switches S_1 and S_2 are in zero current mode. They are turned off by gate signals. The resonant current and capacitor voltage can be expressed as the following equation, where V_T is the AC terminal voltage at this mode.

Initial condition: $i_r = 0$, $v_C = -kV_m$

$$i_r = \frac{1}{Z_r}(kV_m + V_T)\sin\omega_r(t - t_0) \tag{1}$$

$$v_C = V_T - (kV_m + V_T)\cos\omega_r(t - t_0) \tag{2}$$

where $Z_r = \sqrt{\frac{L_r}{C_r}}$, $\omega_r = \frac{1}{\sqrt{L_r C_r}}$

The duration of Mode 1 can be calculated as

$$t_1 - t_0 = \frac{1}{\omega_r}\sin^{-1}\left(\frac{Z_r I_{dc}}{kV_m + V_T}\right) \tag{3}$$

The voltage across the resonant capacitor at t = t_1 is obtained by

$$v_C(t_1) = V_m - \sqrt{(kV_m + V_T)^2 - (Z_r I_{dc})^2} \tag{4}$$

Mode 2 – Capacitor discharge mode

The DC current flows through the DC reactor, and the resonant current flows through S_{r1}, C_r, S_{r2} until the resonant capacitor C_r discharges fully. The resonant current can be expressed as

$$v_C = \frac{1}{C_r}\int_{t_1}^{t} i_r dt + v_C(t_1)$$
$$= \frac{I_{dc}}{C_r}(t - t_1) + v_C(t_1) \tag{5}$$

where $i_r = I_{dc}$

The duration of Mode 2 is obtained by

$$t_2 - t_1 = \frac{-C_r}{I_{dc}} v_c(t_1)$$

$$= \frac{-C_r}{I_{dc}} \left(V_m - \sqrt{(kV_m + V_I)^2 - (Z_r I_{dc})^2} \right) \qquad (6)$$

where $v_c(t_2) = 0$

The time elapsed for reverse voltage across the switch can be derived from equation (6)

$$t_{RV} = \frac{C_r}{I_{dc}} (V_I - v_c(t_1))$$

$$= \frac{C_r}{I_{dc}} \sqrt{(kV_m + V_I)^2 - (Z_r I_{dc})^2} \qquad (7)$$

Mode 3 – Free-wheeling mode

The cell current flows through two paths of S_{r1} - D_{r2} and D_{r1} - S_{r2} with free-wheeling action. The voltage across the resonant capacitor becomes zero, while the reactor current is maintained.

$$i_r = I_{dc}, \quad v_c = 0 \qquad (8)$$

The time elapsed during this mode is negligible. Therefore, it is assumed almost zero.

$$t_3 - t_2 \cong 0 \qquad (9)$$

Mode 4 – Capacitor charging mode

Switches S_{r1} and S_{r2} in soft-switching mode turn off in a zero voltage state. The cell current flows through D_{r1}, C_r, and D_{r2}. The capacitor C_r is slowly charged, and its voltage is expressed as

$$i_r = I_{dc}, \quad v_c = -\frac{I_{dc}}{C_r}(t - t_3) \qquad (10)$$

The time elapsed during this mode is calculated by the following equation.

$$t_4 - t_3 = \frac{C_r k V_m}{I_{dc}} \qquad (11)$$

where $v_c(t_4) = -kV_m$

Mode 5 – Current transition mode

At the end of Mode 4, the capacitor voltage is charged by $-kV_m$. Inverter switches S_3 and S_4 turn on in a zero current state. The commutation circuit is blocked from the main circuit.

Initial condition: $i_r = -I_{dc}, \quad v_c = -kV_m$

$$i_r = -\frac{1}{Z_r}(kV_m - V_I')\sin\omega_r(t - t_4) + I_{dc}\cos\omega_r(t - t_4) \qquad (12)$$

$$v_c = V_I' + (kV_m - V_I')\cos\omega_r(t - t_4) + Z_r I_{dc}\sin\omega_r(t - t_4) \qquad (13)$$
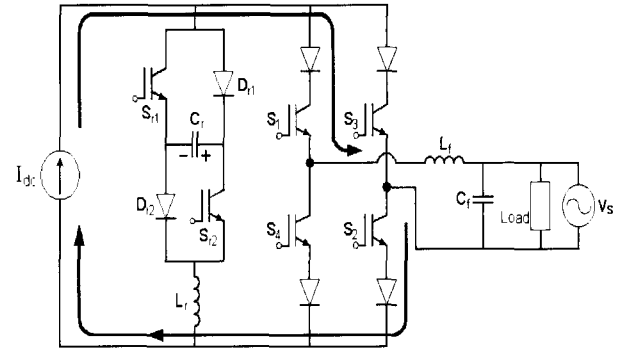
where V'_T is the AC terminal voltage at this mode.

The duration of this current transition mode can be derived as

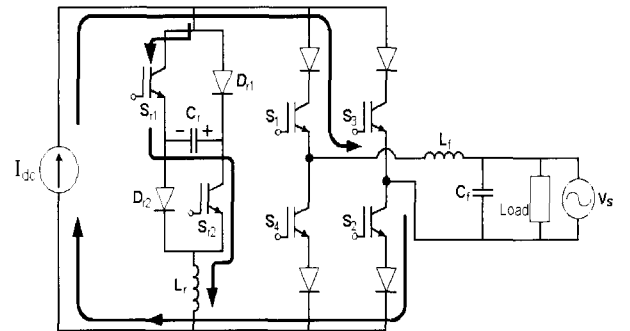$$t_5 - t_4 = \frac{1}{\omega_r}\tan^{-1}\left(\frac{Z_r I_{dc}}{kV_m - V_I'}\right) \qquad (14)$$

where $i_r(t_5) = 0$

Total commutation time can be derived by adding equations (3), (6), (9), and (11).

$$t_5 - t_0 = \frac{1}{\omega_r}\sin^{-1}\left(\frac{Z_r I_{dc}}{KV_m + V_T}\right)$$

$$+ \frac{1}{\omega_r}\tan^{-1}\left(\frac{Z_r I_{dc}}{kV_m - V_I'}\right) + \frac{C_r k V_m}{I_{dc}}$$

$$- \frac{C_r}{I_{dc}}\left(V_m - \sqrt{(kV_m + V_m)^2 - (Z_r I_{dc})^2} \right) \qquad (15)$$

(a) Mode 0

(b) Mode 1

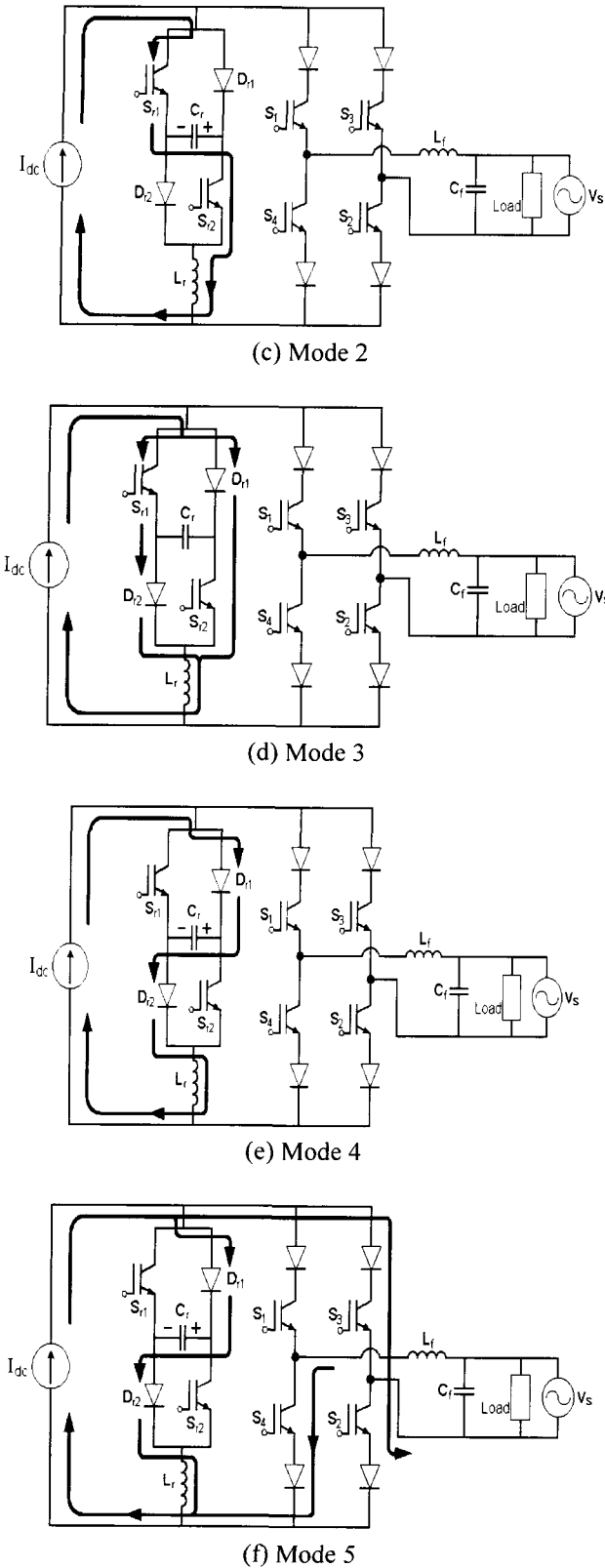(c) Mode 2

(d) Mode 3

(e) Mode 4

(f) Mode 5

Fig. 4 Operation mode of the proposed inverter

The design of the commutation circuit can be implemented considering the detail operation mechanism of each mode. The value of the charge factor k for proper commu-

tation can be determined by the following equation.

$$k \geq 1 + \frac{Z_r}{Z_m} \tag{16}$$

where $Z_m \equiv \dfrac{V_m}{I_{dc}}$

The value of C_r should be determined by considering the maximum dv/dt and di/dt of the switching elements and the maximum resonant commutation time.

The switching pattern to determine the turn-on and turn-off instance of the switching element affects the harmonic level of the output current. Generally, this can be reduced, by increasing the number of pulses within a half period of the power frequency. However, the maximum number of pulses is determined by the switching speed of the switching element and the resonant frequency of commutation circuit.

In this study, a special switching pattern was adopted. The switches in the upper part, S1 and S3, operate in square wave mode, while the switches in lower part, S2 and S4, operate in PWM mode. The PWM pulses are generated by comparing the reference sinusoidal wave with the saw-toothed carrier wave as shown in Fig. 5. The gate pulses for switch S4 are applied by inverting the pulses to switch S2. The pulses for switch S2 are generated when the reference signal is higher than the saw-toothed carrier for one half period, while the pulses for switch S4 are generated when the reference signal is higher than the saw-toothed carrier for another half period.
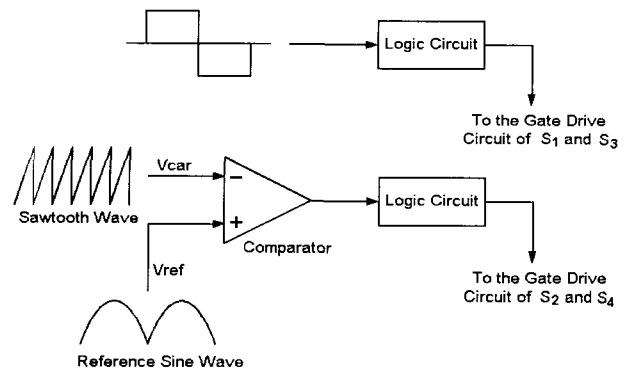

Fig. 5 Gate pulse generation

4. Simulation

Computer simulation with SPICE have verified the feasibility of the proposed soft-switching current-source inverter. The power network used in simulation is exactly the same as that shown in Fig. 3. The circuit parameters used in the simulation are shown in Table 1.

Table 1 Simulation parameters

| Source Voltage	150V $_{rms}$
AC Filter L_f, C_f	5mH, 20μF
Resonant Reactor L_r	18μH
Resonant Capacitor C_r	0.15μF
DC Reactor L_s	500mH

Fig. 6 shows the simulation results. Fig. 6a shows the voltage and current waveforms, which explain the commutation operation. The upper two waveforms show the voltage across switches S1 and S3. The third one shows the resonant pulses for Sr1 and Sr2. The fourth and fifth waveforms show the resonant current and voltage in capacitor. Fig 6b shows the square pulses for switch S1 and S3 and PWM pulses for switch S2 and S4. Fig. 6c shows the snapshot diagram for the turn-on instance of the main switches. It is clear that the switch turns on in a zero-current state. Fig. 6d shows the voltage and current variations of switch S_{r1} in the commutation circuit. It is clear that this switch operates in a soft-switching scheme, too. Fig. 6e shows the voltage and current waveforms in the output terminal of the proposed inverter. Although it contains some harmonics, the output voltage waveform has an envelope of sinusoidal waveform.
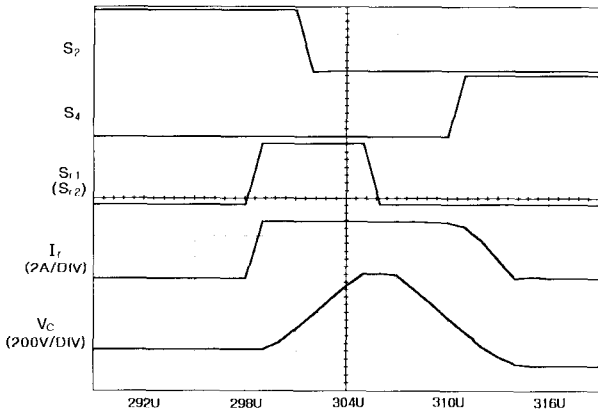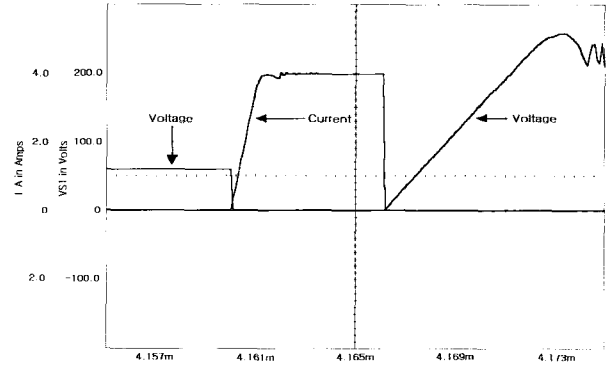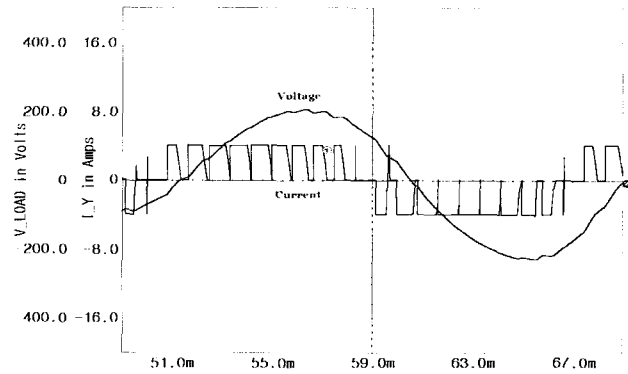

(a) Commutation waveform
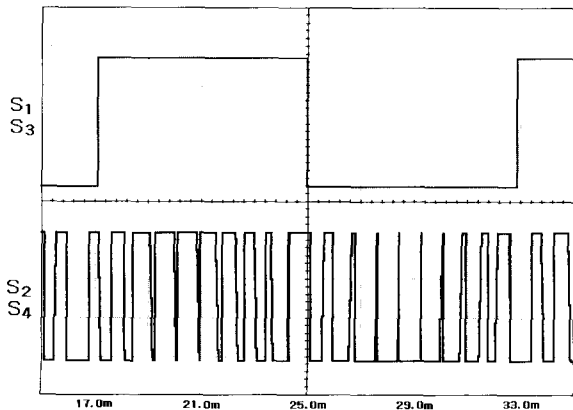
(b) Pulse waveform
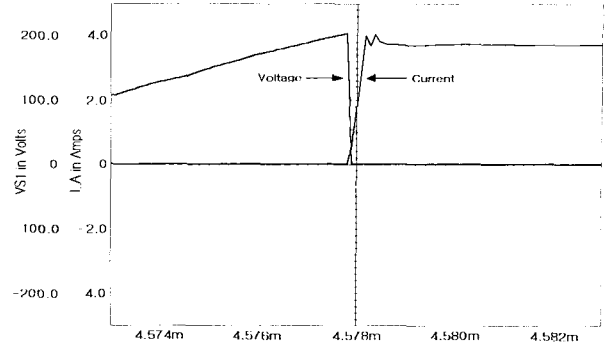
(c) Turn-on transition of switch S_1

(d) Turn-on and turn-off transition of S_{r1}

(e) Output voltage and current

Fig. 6 EMTP simulation results

5. Experimental results

A scaled prototype was built and tested to confirm the feasibility of actual system implementation. Fig. 7 shows the circuit diagram of the scaled prototype, which has a 120V/2kVA rating. The power circuit is composed of six IGBTs and six fast-recovery diodes. A 80C196KC 16-bit microprocessor was used as a main controller for the whole system. The bus voltage of phase A was detected, and the obtained signal was sent to the zero-crossing detector for synchronizing the inverter output voltage with the AC system. The pulses for commutation switches are generated by detecting the falling-edge of pulses for main switches and by using EPLD ipLSI1032.
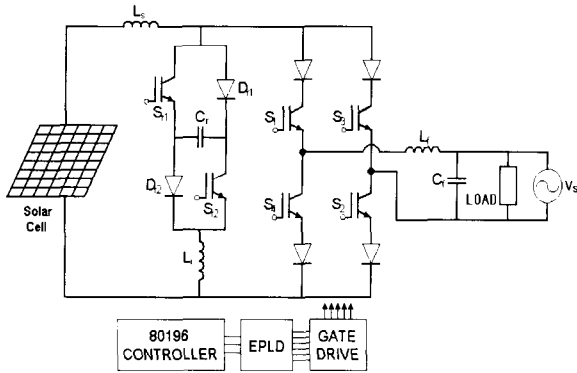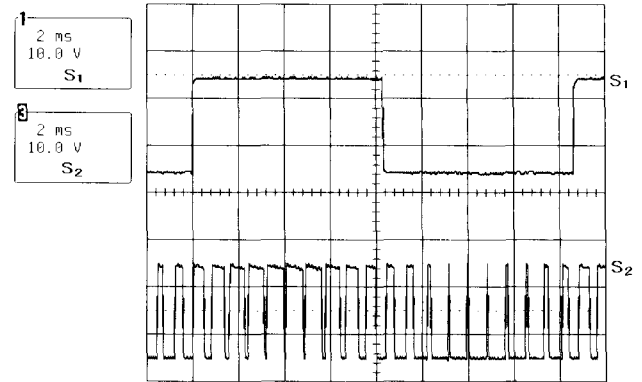
**Fig. 7** Hardware configuration of scaled prototype

Table 2 PV module parameter

Model name	M65(SIEMENS)
Max. output power	43 [Wp]
Open circuit voltage (Voc)	18.0 [V]
Short circuit current (Isc)	3.32 [A]
Voltage at load	14.6 [V]
Amperage at load	2.95 [A]

Eight photovoltaic modules are connected in series to obtain the operation voltage in the experimental work. The ratings of the photovoltaic cell are shown in Table 2.

Fig. 8 shows the experimental results with the prototype explained above. Fig. 8a shows the voltage and current waveforms in the commutation operation, which is very close to the simulation results. Fig. 8b shows two sets of pulses generated for switch S1 and S3 and the PWM gate pulses generated for switch S2 and S4. Fig. 8c shows the snap-shot diagram for the turn on instance of the main switch, which is a very similar shape to that in simulation. Fig. 8d shows the voltage and current variations of the switch in the commutation circuit. It is clear that this switch operates in a soft-switching scheme as verified in simulation. Fig. 8e shows the output voltage and current waveforms of the proposed soft-switching inverter. Although it has some high-frequency harmonics, the output voltage has an envelope of sinusoidal wave.
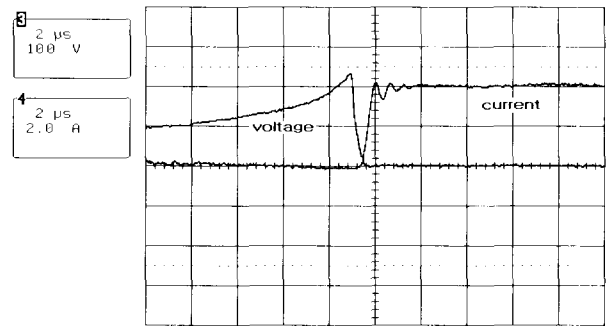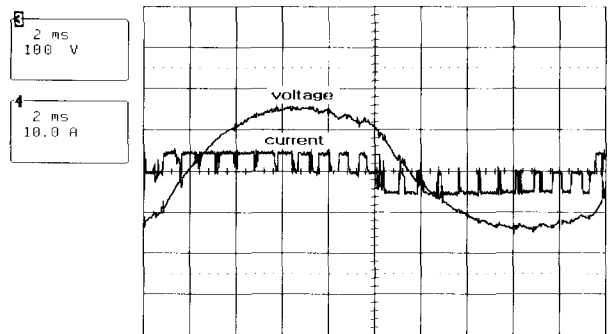
(a) Commutation waveforms

(b) Pulse waveforms

(c) Turn-on transition of switch S_1
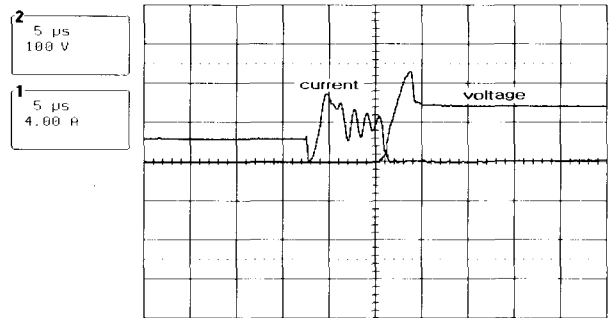
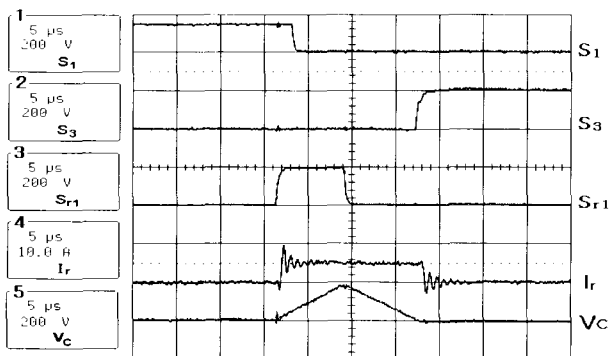(d) Turn-on and turn-off transition of S_{r1}

(e) Output voltage and current

Fig. 8 Prototype experimental results

6. Conclusion

This paper proposes a soft-switching current source in-

verter with an H-type commutation module and analyzes its operation in detail. For theoretical analysis, an equivalent circuit for each operation mode was derived and computer simulations with SPICE were performed to confirm the system operation. A scaled prototype was built and tested to investigate the feasibility of actual system implementation.

Both simulation and experimental results confirm that the proposed system has very low switching stress through a soft-switching scheme. The low switching stress can reduce the switching loss and extend the device lifetime. The proposed soft-switching current source inverter can be used for a solar power system.

Acknowledgement

References

[1] K. Hirachi, K. Matsumoto, "Harmonic Current Reduction Control Scheme Single-phase Current Source-Fed PWM Inverter and Its PV System Application", Proc. PEMC'98, No. 7, pp.59-64, 1998.

[2] Y. Konoshi, E. Hiraki, Y. Matsumoto, Y. L. Feng and M. Nakaoka, "Current-Fed Three-Phase Converter and Voltage-Fed Three-Phase Converter using Optimum PWM Pattern and Their Performance Evaluation", Conf. Rec. of IEEE EPE-Annual Meeting, pp. 2893-2900, 1997.

[3] G. Moschopoulos and G. Joos, "A Novel Soft-Switched PWM Current Source Rectifier/Inverter", Conf. Rec. of IEEE PESC-Annual Meeting, 1997, pp. 573 -579.

[4] G. Hua and F. C. Lee, "Soft-Switching Techniques in PWM Converter", IEEE IECON 1993, pp.637-643.

[5] S. Baek and B. Han, "New Reactive-Power Compensator using Thyristor Current Source Inverter", KIEE Trans. on Electrical Engineering, Vol. 48B, No. 4, pp. 219 -225, April, 1999.

Byung-Moon Han
He received the B.S degree in Electrical Engineering from Seoul National University, South Korea, in 1976 and the M.S and Ph.D. degrees in Electrical Engineering from Arizona State University, in 1988 and 1992, respectively.
He was a senior research engineer with Science and Technology Center of Westinghouse Electric Corporation, Pittsburgh, PA. Currently, he is a professor in the Department of Electrical Engineering, Myongji University, South Korea. His research interests include high-power electronics and FACTS.

Hee-Jung Kim
He received the B.S. and M.S. degrees in Electrical Engineering from Myongji University, Yongin, Kyunggi-do, South Korea, in 1997 and 1999, respectively. He is currently pursuing the Ph.D. degree in Electrical Engineering from Myongji University. His research interests include power electronics applications for FACTS and custom power.

Seung-Taek Baek
He received the B.S. and M.S. degrees in Electrical Engineering from Myongji University, Yongin, Kyunggi-do, South Korea, in 1997 and 1999, respectively. He is currently pursuing the Ph.D. degree in Electrical Engineering from Myongji University. His research interests include power electronics applications for FACTS and custom power.